Neurochemistry International 131 (2019) 104543

Contents lists available at ScienceDirect

Neurochemistry International

journal homepage: www.elsevier.com/locate/neuint

# Striatal overexpression of β-arrestin2 counteracts L-dopa-induced dyskinesia in 6-hydroxydopamine lesioned Parkinson's disease rats

Zeng-Rui Zhang[a,1], Xing-Ru Zhang[a,1], Xiao-Qian Luan[a], Xin-Shi Wang[a], Wen-Wen Wang[b], Xiao-Yi Wang[c], Bei Shao[a,**], Cheng-Long Xie[a,*]

[a] Department of Neurology, The First Affiliated Hospital of Wenzhou Medical University, Wenzhou, 325000, China
[b] The center of Traditional Chinese Medicine, The Second Affiliated Hospital and Yuying Children's Hospital of Wenzhou Medical University, 325027, Wenzhou, China
[c] Department of Nephrology, The First People's Hospital of Huzhou, Zhejiang, 313000, PR China

ARTICLE INFO

*Keywords:*
β-arrestin2
GPCR
D1R signaling
Parkinson's disease
L-dopa–induced dyskinesia

ABSTRACT

Prolonged administration of Levodopa (L-dopa) therapy can generate L-dopa–induced dyskinesia (LID). Accumulating evidence indicates that hyper-activation of the dopamine D1 receptor (D1R) and the cAMP signaling cascade in the medium spiny neurons (MSNs) of the striatum are involved in LID. Previous studies have shown that striatal β-arrestin2 overexpression significantly reduces LID severity and have indicated that β-arrestin2 may play a causal role in the dyskinesia sensitization process. L-dopa-induced changes in the expression of signaling molecules and other proteins in the striatum were examined immunohistochemically and by western blot. A rAAV (recombinant adeno-associated virus) vector was used to overexpress and ablate β-arrestin2. We found that striatal overexpression of AAV-mediated β-arrestin2 produced less severe AIMs (abnormal involuntary movements) in response to L-dopa, whereas selective deletion of β-arrestin2 in the striatal neurons dramatically enhanced the severity of dyskinesia induced by L-dopa. Furthermore, no significant improvements in motor behavior (FFT: forelimb functional test) were seen with the inhibition or overexpression of β-arrestin2. Finally, overexpression of β-arrestin2 diminished L-dopa-induced D1R and phosphor-DARPP32/ERK levels. Viral deletion of β-arrestin2 markedly enhanced the key biochemical markers in the direct pathway. We found that increased availability of β-arrestin2 ameliorated dyskinesia severity with no influence on the anti-Parkinsonian action of L-dopa, suggesting a promising approach for controlling LID in Parkinson's disease. In addition, overexpression of β-Arrestin2 prevented the development of LID by inhibiting G protein-dependent D1R and phosphor-DARPP32/ERK signaling in dyskinetic rats.

## 1. Introduction

Parkinson's disease (PD) can be relieved by dopamine (DA) precursor Levodopa (L-dopa), which efficiently counteracts the motor symptoms of the disease, i.e., tremor, rigidity, and hypokinemia (Cotzias et al., 1967; Antonini and Tinazzi., 2015). However, prolonged administration of L-dopa therapy can generate L-dopa–induced dyskinesia (LID), affecting approximate 50% of patients in the first 5 years of L-dopa therapy and 90% of patients after 10 years (Stocchi et al., 2008). LID limits the therapeutic efficacy of L-dopa and disrupts quality of life in PD patients (Schaeffer et al., 2014). The development of LID has been attributed to plasticity in pre- and post-synaptic receptor and transporter functions in the striatum (Mosharov et al., 2015). Among these functions, accumulating evidence indicates that chronic L-dopa treatment results in persistent and intermittent hyper-activation of the dopamine D1 receptor (D1R) and the cAMP signaling cascade in the medium spiny neurons (MSNs) of the striatum, which are involved in LID (Feyder et al., 2011). Consequently, pharmacological or genetic interventions aimed at reducing abnormal sensitizing of the D1R may be a potential alternative approach to controlling LID. The sensitization of the D1R produced by dopamine depletion is reflected by the large increase in DARPP-32 phosphorylation, which was observed in response to the administration of L-dopa. L-dopa-induced activation of the cAMP/DARPP-32 cascade has been related to the occurrence of LID (Feyder et al., 2016). Santini et al. reported that increased phosphor-DARPP-32 has been shown to persist for up to 3 months with chronic L-

* Corresponding author.
** Corresponding author.
*E-mail addresses:* M13456063663@163.com, shaobeiwy@163.com (B. Shao), cl_xie1987@sohu.com, Xiechenglong1987@126.com (C.-L. Xie).
[1] These authors contributed equally to this work.

https://doi.org/10.1016/j.neuint.2019.104543
Received 11 July 2019; Received in revised form 16 August 2019; Accepted 2 September 2019
Available online 03 September 2019
0197-0186/ 

dopa administration, suggesting that DARPP-32 is involved not only in the development but also in the maintenance and expression of LID (Santini et al., 2010). Evidence obtained in several models indicates that LID is coupled with increased levels of phosphor-ERK (Pavón et al., 2006). It has been shown that some substances can promote D1R transmission and phosphorylate ERK via the activation of the PKA/DARPP-32 signaling cascade (Valjent et al., 2005). ERK activation facilitates the expression of the FosB transcription factor and p-Ac-H3, which are also implicated in LID. In addition, dyskinesia is related to ERK-dependent activation of mTORC1, which is likely to accelerate local protein synthesis (Brugnoli et al., 2016). In summary, phosphor-DARPP-32 and ERK are both key markers in the D1R signaling pathway in LID that can reflect the activation of D1R sensitization.

The arrestin family includes the following four members: β-arrestin1, β-arrestin2, x-arrestin, and s-arrestin. These proteins are cytosolic proteins that regulate G protein-coupled receptor (GPCR) desensitization internalization, trafficking, and signaling in a GPCR kinase (GRK)-dependent manner (Lohse et al., 1990; Lee et al., 2016). β-arrestin2, as a non-visual arrestin, can transduce GPCR signals by forming protein complexes with signaling molecules downstream of G proteins to mediate GPCR desensitization, degradation and recycling (Zhan et al., 2011). GPCR signaling is strictly controlled by this process, and altered β-arrestin2 expression has been reported in cancers, cardiovascular diseases, and neurodegenerative diseases (Bohn et al., 2003; Bruns et al., 2006). Although β-arrestin2 can transduce multiple signals in cells, little is known about its participation in PD or LID. To date, only one study reported that β-arrestin2 overexpression significantly reduced LID while maintaining the therapeutic effect of L-dopa in knock-out PD mice (Urs et al., 2015). Therefore, we reason that β-arrestin2 can influence several pathways implicated in LID, and activated β-arrestin2 may reduce LID performance. However, it is not known whether the mechanism is by reducing abnormal sensitizing of the D1R or lowering the level of the D1R signaling molecules in an established model of LID.

In the present study, we mainly investigated the effect of genetic overexpression/deletion of β-arrestin2 in the striatum on abnormal involuntary movements (AIMs) and motor function. In parallel, we evaluated the molecular mechanisms associated with the anti-dyskinetic effects of β-arrestin2. We used unilateral 6-hydroxydopamine (6-OHDA)-lesioned rats to study the development of LID. In addition, we investigated phosphor-DARPP32 and phosphor-ERK activation in the striatum after the deletion and overexpression of β-arrestin2.

## 2. Materials and methods

### 2.1. Animals

All studies were approved through the Ethical Committee of Wenzhou Medical University (Wenzhou, China). Ninety-two adult male Sprague-Dawley (SD) rats (no predetermined sample size calculation was performed) weighing 180–250 g were used in this study and were supplied by the Wenzhou Medical University animal facility (Wenzhou, China). The number of rats in each group is indicated in the figure legends, and all rats were housed with a maximum of four per cage on a 12/12 h light/dark cycle and comfortable temperature of 22–26 °C with water and food available ad libitum. Animals had at least one week for acclimatization before the stereotaxic procedure. All experimental protocols involving the animals were reviewed and approved by the Ethical Committee of the Medical School of Wenzhou Medical University. All procedures were carried out in accordance with the approved guidelines and regulations of the National Institutes of Health for the care and use of laboratory animals (NIH publication No. 80-23).

### 2.2. Virus construction and preparation

In this study, the overexpression of β-arrestin2 was based on the construction of recombinant adeno-associated virus (AAV) expression vectors (Obio Technology Corp, Shanghai, China) carrying pAAV-CMV-EGFP-2A-Arrb2-3FLAG (arrestin, beta2, Arrb2 [Rat], 1233 bp). Briefly, complete plasmid DNA (pAAV-CMV-EGFP-2A-MCS-3FLAG) was digested from the cleavage site Nhe I to BamH I, and the targeting genes of Arrb2 was packaged into the section. The constructed plasmid and complete plasmid were packaged into AAV, and the final virus titer was 1.37E + 13 v.g./ml. The titer used in the study was diluted to 1.37E + 12 v.g./ml and evaluated for infectivity in HEK 293T cells. To silence β-arrestin2 expression, we generated a shRNA against rat β-arrestin2 and a luciferase shRNA as a negative control. These were also packaged into AAV vectors using a two-plasmid system in HEK 293 cells. The viruses were administered into the striatum via a stereotaxic injection to generate unilateral 6-OHDA lesioned rat models. In brief, PD models were selected on the day following apomorphine and anesthetized and placed in a stereotaxic frame. The coordinates were calculated using the rat brain atlas as follows: 1) anterior-posterior (AP), + 0.9 mm, medial-lateral (ML), − 4.5 mm, dorsal-ventral (DV), − 5.0 mm relative to the Bregma and 2) AP, + 0.5 mm, ML, − 2.5 mm, DV, − 4.2 mm according to the rat brain atlas. Viruses containing overexpressed/ablation β-arrestin2 vector groups (AAV-β-arrestin2-EGFP and AAV-sh. β-arrestin2, respectively) and AAV empty vector groups were infused at a rate of 0.1 μl/min for 10 min (final volume 1.0 μl/site), and the microsyringe was held in place for an additional 10 min before being slowly withdrawn.

### 2.3. Induction of L-dopa-induced dyskinesia (LID)

Surgery was conducted as described before (Xie et al., 2016). The rats were anesthetized with 1% pentobarbital sodium (40 mg/kg, i.p.) and were installed on a stereotaxic apparatus. The stereotaxic procedure was carried out according to our previous experiment, and unilateral 6-OHDA-lesioned rat models of PD were created as follows (Xie et al., 2014). First, 6-OHDA hydrochloride (32 μg dissolved in 8 μL) containing 0.2% ascorbic acid for PD and 0.9% physiological saline for the sham group were infused into the right medial forebrain bundle (MFB) at a constant rate of 1 μl/min using the following coordinates: 1) AP, − 4.4 mm, ML, − 1.2 mm, DV, − 7.8 mm; 2) AP, − 3.7 mm, ML, − 1.7, DV, − 7.8. The tooth bar was set to − 2.4 mm. Three weeks after surgery, rats were screened by rotation after the use of apomorphine (APO, 0.5 mg/kg, i.p.), and the rats displaying more than 7 full body turns/min toward the opposite side of the lesioned side were selected for induction of LID. All successful PD rats were divided into groups of PD injected with 0.9% physiological saline and PD injected with LID with L-dopa (15 mg/kg, i.p.) and Benserazide (3.75 mg/kg, i.p.) twice-daily (9:00 a.m. and 15:00 p.m.) for 3 weeks as described in our previous paper (Xie et al., 2014).

### 2.4. Drugs and treatment

L-dopa (15 mg/kg, i.p.), Benserazide (3.75 mg/kg, i.p.) and 6-OHDA (32 μg dissolved in 8 μL) were purchased from Sigma-Aldrich Co. Ltd. (St. Louis, USA) and were freshly prepared in saline containing 0.2% ascorbic acid. Apomorphine hydrochloride (0.5 mg/kg, i.p.) was purchased from Wako Co. Ltd. (Japan) and dissolved in saline with 0.2% ascorbic acid before use and was administered by intraperitoneal injection at a volume of 2 ml/kg.

### 2.5. AIM ratings and forelimb functional test (FFT)

The rats were monitored for AIMs in a clear plastic case individually from the first day treated with steady doses of L-dopa and Benserazide for 21 days, and then rats were injected with AAV for three weeks. The rats were randomly divided into the AAV or control group to guarantee that LID expression was equivalent prior to the second surgery. AIMs were assessed twice a week by a trained observer in a blind manner after drug treatment at 20-min intervals for a total of 120 min. AIMs

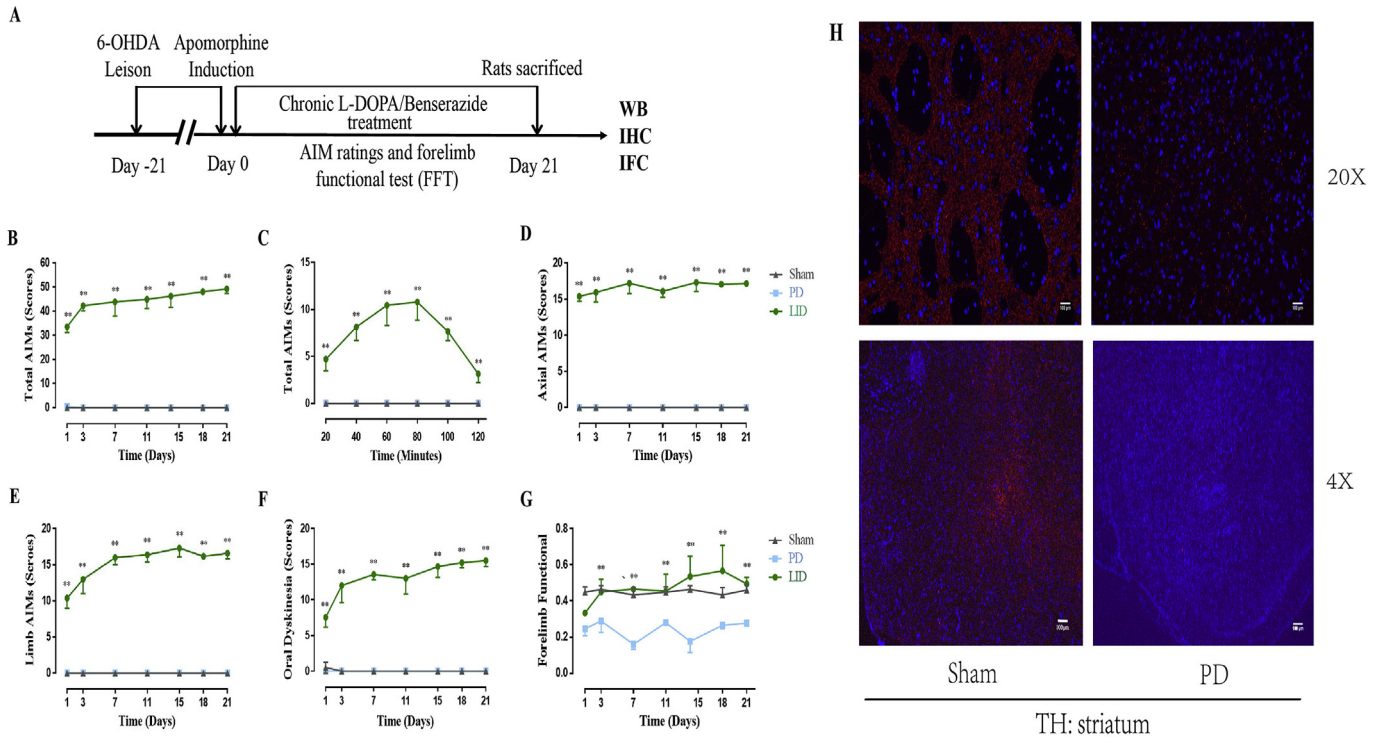


**Fig. 1.** AIMs induced by chronic L-dopa administration. (A) Timeline of experiments. Studies began for SD rats with unilateral 6-OHDA lesions of the nigrostriatal pathway followed by apomorphine screening for selection of animals with complete lesions and sham group (n = 8). Rats in the LID group (n = 8) were administrated once-daily (9:00 a.m.) with L-dopa (15 mg/kg, i.p.) plus benserazide (3.75 mg/kg, i.p.) for 3 weeks. Additionally, rats in the PD group (n = 8) and sham group (n = 18) were treated physiological saline for 3 weeks. AIMs were assessed during this period on days 1, 3, 7, 11, 15, 18 and 21. The animals were sacrificed 2 h after the last injection for WB, IHC and IFC. (B–C) Total AIM score; (D) axial AIM score; (E) limb limb; (F) orolingual AIM score; (G) Forelimb functional test; (H) Extent of the dopaminergic denervation induced by 6-OHDA lesions in each groups in the striatum (4* and 20*, respectively). Data are presented as mean ± standard error; ** $p < 0.01$ vs sham group.

were observed for three areas (axial, limb and orolingual movements) on a severity score scale from 0 to 4 (Cenci et al., 1998): 0 was no AIMs, 1 was infrequent AIMs occurring < 50% of the time, 2 was frequent AIMs occurring > 50% of the time, 3 was constantly present AIMs interrupted by external stimulation (tap on the cage), and 4 was constant AIMs insensitive to external stimulation. Therefore, the maximum theoretical score per monitoring session was 4 × 3*6 = 72. For the FFT (Schallert et al., 2000), rats were placed in a glass cylinder 22 cm in diameter and 35 cm high to record forelimb use during vertical exploration for 5 min (4 intervals over 20 min). We used the same dose of L-dopa (15 mg/kg) and Benserazide (3.75 mg/kg) when performing the cylinder test. Indeed, that dose of L-dopa/Benserazide created obvious AIMs and influenced the accuracy of the cylinder test. Consequently, to avoid AIMs of the fastigium, FFT was carried out 90 min after L-dopa/Benserazide was administered. In the cylinder test described previously, the number of forelimb touches to the cylinder wall was counted by an observer twice a week while the animals moved freely in the cylinder. Forelimb function was expressed as use of the contralateral forelimb of the side lesioned with 6-OHDA as the percentage of the total number of bilateral contacts. Therefore, preferential use of the paw ipsilateral to the lesion (controlled by the intact hemisphere) is indicative of a Parkinsonian defect. L-dopa administration enhances the use of the contralateral paw, controlled by the lesioned hemisphere and is a measure of the anti-Parkinsonian effect of the drug.

### 2.6. Western blot

Two hours after the last drug administration, all rats were decapitated under 1% pentobarbital sodium, and their brains were immediately collected. The two-tailed corpus striatum with a radial pattern was removed in EP tubes on dry ice. Lesioned striatal tissues were homogenized in protein extraction mixed solution comprising RIPA Lysis Buffer, freshly added protease inhibitor cocktail (solarbio) and 100 mM PMSF (Beyotime Institute of Biotechnology). The prepared supernatant was placed in new tubes after centrifugation at 12,000 × *g* for 5 min at 4 °C, and total and membrane-enriched proteins were collected. Then, protein quantity was determined by the BCA protein determination method. Experimental corpus striatum samples (35 μg of protein) from every rat from each treatment group were loaded onto 8–12% sodium dodecyl polyacrylamide gels. Briefly, SDS-PAGE electrophoresis was used to separate the protein, and the proteins were transferred to Polyvinylidene Fluoride (PVDF, pore size: 0.45 μm) membranes. The membrane was blocked with 5% milk in Tris-buffered saline–Tween 20 and incubated with primary antibodies overnight at 4 °C, including polyclonal rabbit anti-Tyrosine Hydroxylase antibody (1:1000; Millipore, *No.ab152*), polyclonal goat Anti-Beta Arrestin2 (1:1000; Abcam, *No.ab31294*), monoclonal rabbit anti-ERK1/2 [1:1000; Cell Signaling Technology (CST)], monoclonal rabbit anti-phosphor-ERK (pT202/pY204, 1:1000; CST), monoclonal rabbit anti-DARPP32 (1:1000; CST), polyclonal rabbit anti-phosphor-DARPP32 (Thr34) (1:1000; Sigma-Aldrich), mouse monoclonal D1R antibody (1:1000; Santa Cruz Biotechnology, *NO.sc-33660*), mouse monoclonal D2R antibody (1:1000; Santa Cruz Biotechnology, *NO.sc-5303*) and polyclonal rabbit anti-GAPDH antibody (1:5000; Bioworld Technology). Then, the membrane was incubated with anti-rabbit or goat horseradish peroxidase IgG (1:1000; Beyotime Institute of Biotechnology) for 1 h at room temperature after washing 3 times using Tris-buffered saline–Tween 20 and immunoreactive bands quantified based on a secondary binding chemiluminescence detection system via Quantity One software (Image Lab, Bio-Rad).

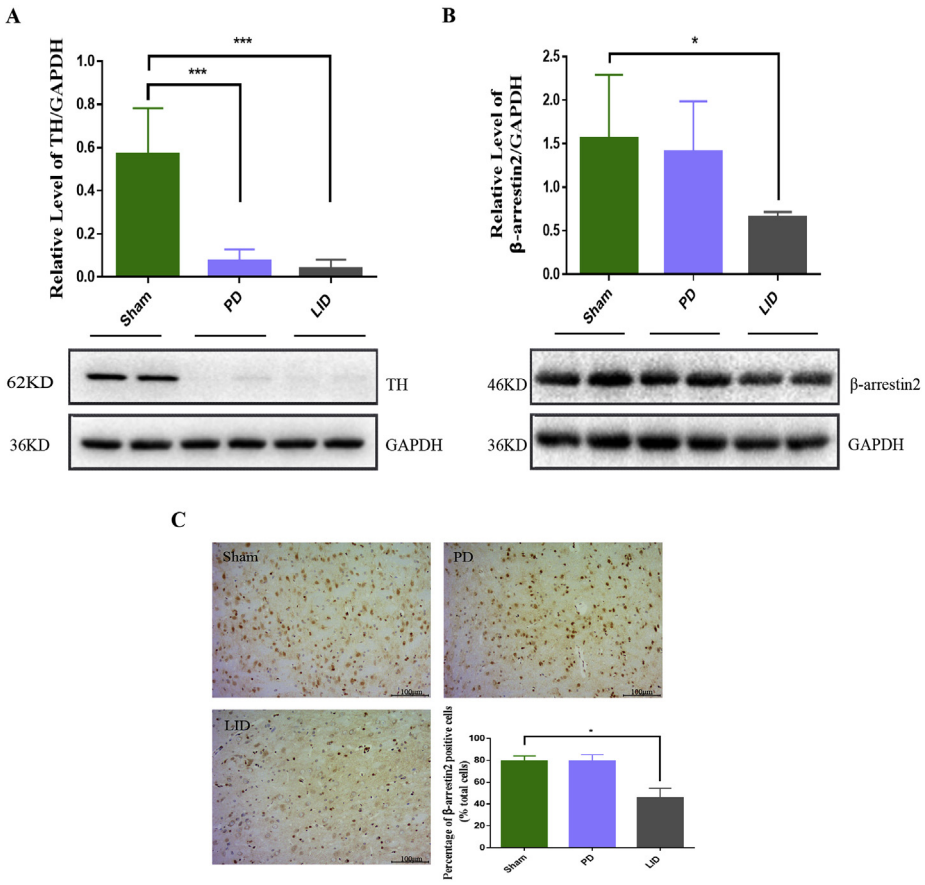


**Fig. 2.** Protein levels and positive neurons were evaluated by WB or IHC from the ipsilaterally striatum of the rat brains. (A) Tyrosine hydroxylase (TH) protein level was dramatically decreased by nearly 80%–90% in the PD or LID rats when compared with sham group. (B) β-arrestin2 expression relative to actin level in three groups; (C) β-arrestin2 positive neurons in striatum. Shown is a coronal section of the striatum from the lesioned hemisphere. * $p < 0.01$ vs sham group; # $p < 0.05$ vs sham group (ANOVA followed by Bonferroni post hoc tests).

### 2.7. Immunohistochemistry (IHC) and immunofluorescence (IFC)

The rats were sacrificed 2 h after the last L-dopa injection and behavioral test via decapitation and perfused transcardially with 0.9% NaCl followed by cold 4% formaldehyde. The rat brains were kept intact, prepared in 4% formaldehyde (4 °C), and then soaked in 10%, 20%, 30% sucrose in turn so they sank to the bottom. Brains were frozen and stored at −80 °C until frozen sectioning. A microtome-cryostat cut 5–8 μm thick coronal rat brain sections, which were collected and processed for IHC and IFC. For IHC experiments, brain sections were then added to 3% hydrogen peroxide to bind the endogenous peroxidase. For antigen retrieval, the sections were rinsed (3 × 5 min) in 0.1 M PBS and transferred to 10 mM sodium citrate solution while gently stirring at 80 °C for 30 min. The sections were incubated overnight at 4 °C with the primary antibodies, goat β-Arrestin2 (1:200; Abcam, *No.ab31294*) and rabbit anti-Tyrosine Hydroxylase (1:200; Millipore, *No. ab152*). After rewarming for 45 min at 37 °C and washing in PBS 3 times, brain sections were incubated for 1 h in secondary antibody (diluted 1:200; Beyotime Institute of Biotechnology) and then colored in DAB mixed solution. Image acquisition was performed using a microscope, and the tissue signal was quantified using Image-Pro Plus 6.0. To count positive cells in the striatum, the sample area was selected through a 20 × objective on the microscope. In addition to counting positive cells in each sample area, Image Pro Plus 6.0 software provides information about the number of pixels and optical density (OD) values. Then, we compared the values for different groups according to the formula: area covered by the cell average OD value/unit area (Lundblad et al., 2003). In terms of IFC, striatum sections were incubated overnight at 4 °C in the primary antibody solution, rabbit anti-Tyrosine Hydroxylase (1:200; Millipore, *No. ab152*). Then, following washing with PBS 3 times, slices were incubated in the dark in FITC-conjugated goat anti-rabbit IgG (1:1000, Beyotime Institute of Biotechnology) at room temperature for 1 h. Finally, the sections were mounted using anti-fluorescent quenching solution and observed under a fluorescence microscope.

### 2.8. Statistical analysis

Data were expressed as the mean ± standard deviation (SD). The behavioral measurements for AIMs and the FFT were nonparametric and were analyzed using Kruskal Wallis tests followed by Dunn's test for multiple comparisons if comparing data over multiple days or Mann–Whitney U tests. Neurochemical data conformed to a normal distribution and were analyzed by one-way analysis of variance (ANOVA) followed by Bonferroni multiple comparison post-hoc tests. $P < 0.05$ was considered significant. We utilized dot-plots or box-plots instead of simple bar graphs with small sample sizes ($n < 15$). Data were analyzed using Graphed Prism (Graph-Pad, La Jolla, California) or SPSS 17.0.

## 3. Results

### 3.1. Striatal β-arrestin2 is downregulated in parkinsonian rats after repeated L-dopa administration

Fig. 1A shows the experimental design of the first part of the study. To imitate the generation of abnormal movements in PD by repeated L-dopa administration, we used a well-established hemi-Parkinsonian rat model generated by unilateral injection of the neurotoxin 6-OHDA into the MFB. The 6-OHDA-lesioned PD rats treated with L-dopa plus Benserazide alone for 21 days following standardized protocols developed dyskinesia as manifested by increasing AIM scores for total (Fig. 1B and C), axial (Fig. 1D), limbs (Fig. 1E) and orolingual (Fig. 1F) muscles with time. The sham and 6-OHDA-lesioned PD groups received saline for 21

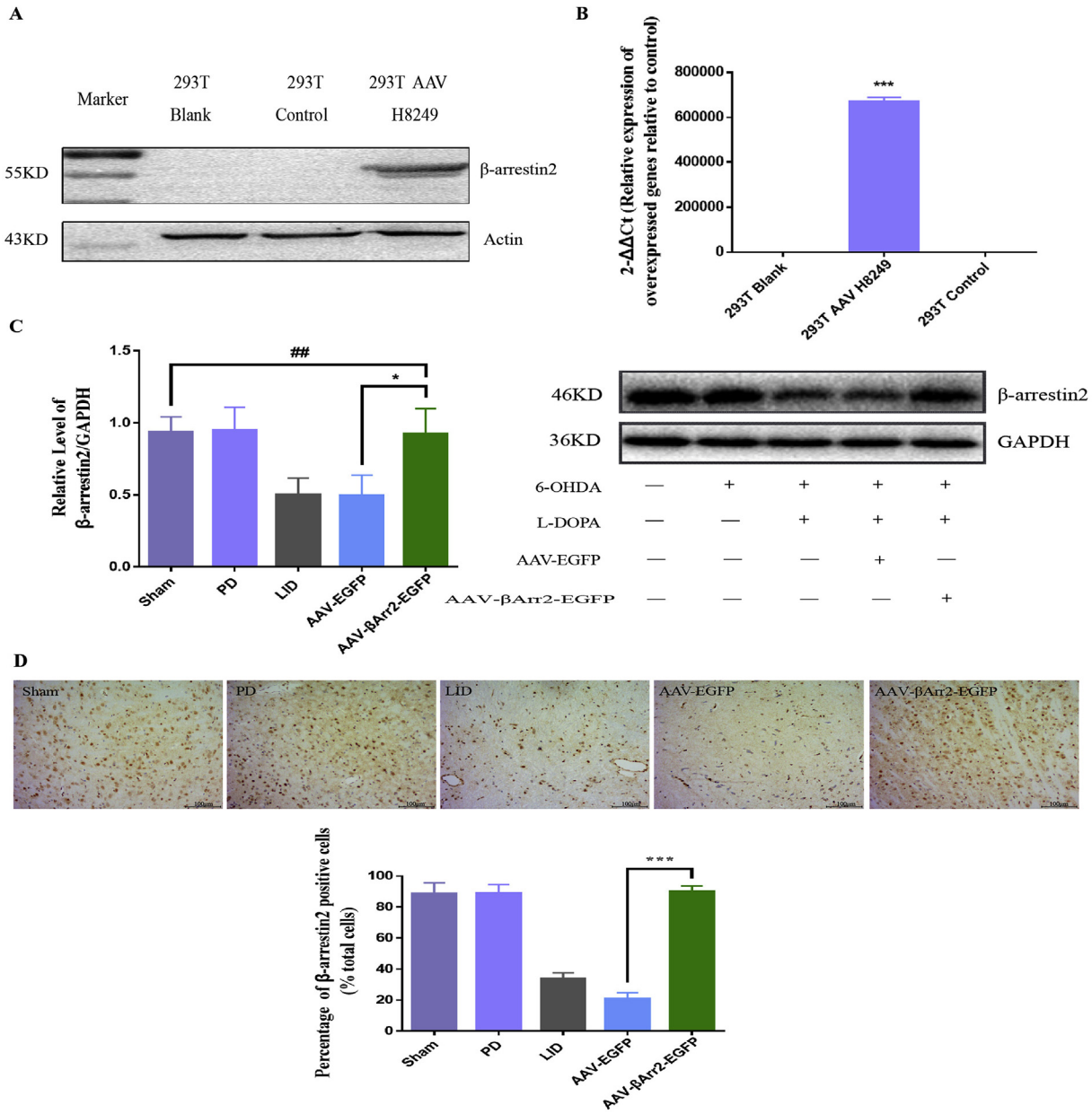


**Fig. 3.** Recombinant adeno-associated virus-induced (AAV) β-arrestin2 expression in vitro and *in vivo*. AAV-β-arrestin2 (H8249) showed one of the most focalized transduction patterns. (A) Detection of the AAV-β-arrestin2 expression by WB in vitro; (B) Detection of the AAV-β-arrestin2 expression by Q-PCR in vitro; (C) Detection of the AAV-β-arrestin2 expression by WB in the lesioned striatum in animals; (D) Detection of the AAV-β-arrestin2 expression by IHC in the lesioned striatum in animals. AAV-β-arrestin2 can increase the β-arrestin2 proteins and immunopositive neurons compared with other groups (ANOVA followed by Bonferroni post hoc tests).

days and did not develop LID symptoms, and the median ALO AIM score ranged from 0 to 2 ($p < 0.01$ vs LID group, Fig. 1). We observed that PD rats treated with L-dopa preferred to use the compromised (contralateral) forelimb to touch the inner wall of the cylinder compared with the PD rats treated with saline ($p < 0.01$, Fig. 1G). The extent of 6-OHDA-induced dopamine alteration was verified by IFC and WB with an antibody raised against Tyrosine hydroxylase (TH). TH-positive neurons in the striatum and protein levels were dramatically decreased by nearly 80%–90% in the PD and LID rats compared with those in the sham group ($p < 0.05$, Figs. 1H and 2A). We analyzed the level of β-arrestin2 protein in the striatum on the side of the 6-OHDA injection in each group. Fig. 2B illustrated the striatal expression of β-arrestin2 following unilateral dopamine depletion. There was a marked reduction in β-arrestin2 expression in the dopamine-depleted striatum of rats treated with L-dopa ($p < 0.01$, Fig. 2B). Analogously, we found an identically striking decrease in β-arrestin2 immunostaining in the LID group compared with the PD or sham group ($p < 0.01$, Fig. 2C). These findings from the IHC method were thus consistent with our observations with WB. There were also perceptible decreases in β-arrestin2 protein and immunostaining of positive neurons in PD group compared to those in the sham group ($p < 0.01$, Fig. 2B and C).

### *3.2. AAV-mediated β-arrestin2 overexpression decreases AIMs induced by L-dopa in hemi-parkinsonian rats with no influence on the anti-parkinsonian activity of L-dopa*

We constructed AAV-encoding EGFP (control) or rat β-arrestin2 tagged with EGFP for easy detection. The infectivity of AAV-β-arrestin2-EGFP was evaluated in 293T cells (Fig. 3A and Fig. 3B). The choice of AAV serotype was guided by evidence from cell cultures

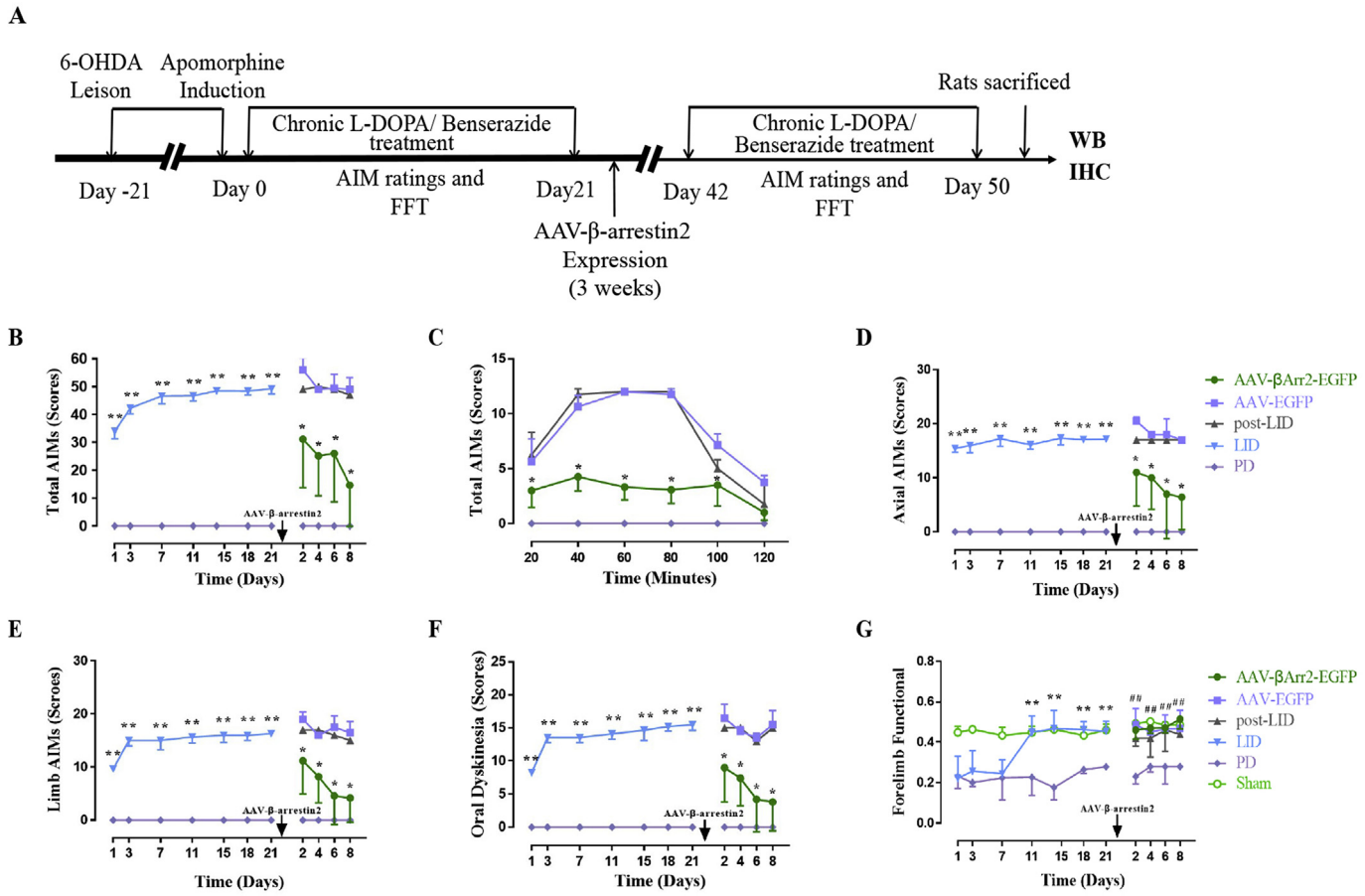


**Fig. 4.** AAV-Mediated β-arrestin2 overexpression in striatum decrease AIMs induced by L-dopa in 6-OHDA lesioned rats. (A) The protocol of the second part experimental design; (B–C) Total AIM score; (D) axial AIM score; (E) limb AIM score; (F) orolingual AIM score; (G) Forelimb functional test. Thus, we found the enhanced availability of β-arrestin2 alleviated already established LID in terms of AIM score without reducing the active effects of L-dopa on parkinsonian motor scores. ** $p < 0.05$ vs PD group; ## $p > 0.05$ vs LID group ($n = 6$ for each groups, Kruskal Wallis followed by Dunn's test for multiple comparisons).

indicating that AAV-β-arrestin2-EGFP (H8249) showed one of the most focalized transduction patterns in vitro. β-arrestin2 protein and mRNA expression were significantly increased by AAV-β-arrestin2 (H8249) transduction in the 293T cells compared to transduction of the control AAV-EGFP (Fig. 3A and B). Similarly, in the rat's dorsal striatum, we found AAV-β-arrestin2-EGFP increased the β-arrestin2 proteins (Fig. 3C) and immunopositive neurons (Fig. 4D) compared with other groups. Fig. 4A shows the second part of the experimental design. Because anti-dyskinetic action is required LID patients, we tested whether overexpression of β-arrestin2 would influence pre-existing dyskinesia performance. Behavioral evaluations in response to L-dopa started the day before stereotaxic infusion of AAV-β-arrestin2 or AAV-EGFP vectors to obtain baseline scores and resumed 21 days after viral infusion. PD rats treated with L-dopa for three weeks developed a progressive increase in LID as indicated by AIMs before injection of β-arrestin2 or control viruses. AAV-β-arrestin2-EGFP injected rats exhibited ALO AIMs that were markedly reduced from week 3 to week 4 post-surgery compared with pre-surgery score ($p < 0.01$, Fig. 4B and C). Similarly, we found the same trend in axial AIMs ($p < 0.01$, Fig. 4D), limb AIMs ($p < 0.01$, Fig. 4E) and orolingual AIMs ($p < 0.01$, Fig. 4F). Thus, the enhanced availability of β-arrestin2 alleviated already established LID. To rule out the possibility that the anti-dyskinetic effect in AAV-β-arrestin2-EGFP rats was due to locomotor impairment, we next sought to determine whether the AAV-β-arrestin2-EGFP injection influenced the therapeutic response to L-dopa. We observed that PD rats treated with L-dopa preferred to use the contralateral forelimb to touch the inner wall of the cylinder in the FFT ($p < 0.05$, Fig. 4G). If the animals were co-injected with AAV-β-arrestin2-EGFP or AAV-EGFP, the rats also demonstrated similar FFT scores to the LID group ($p > 0.05$, Fig. 4G). Taken together, these results indicated that striatal expression of β-arrestin2 alleviated LID severity without reducing the active effects of L-dopa on Parkinsonian motor scores.

### *3.3. AAV-mediated β-arrestin2 overexpression blocks L-dopa-induced D1R and phosphor-DARPP32/ERK signaling in the lesioned striatum*

To discover the potential molecular mechanisms underlying the effects of AAV-β-arrestin2 on LID, we analyzed the expression of components of the D1R signaling pathway, such as the D1R and phosphor-DARPP32/ERK, in the DA-denervated striatum. These markers proved to be key markers in the appearance of D1 dopamine receptor supersensitivity in LID. In PD rats treated with L-dopa, the level of striatal DR1 protein expression in the lesioned hemispheres was significantly increased compared to the other five groups (Fig. 5A). This elevation in DR1 expression was apparently prevented in animals treated with AAV-β-arrestin2-EGFP rather than AAV-EGFP. The level of DR2 was decreased in LID rats but not changed by AAV-β-arrestin2 or AAV-EGF (Fig. 5A). In addition, western blotting showed that repeated treatment with L-dopa resulted in significant phosphor-DARPP32/ERK expression in the lesioned striatum in the LID group ($p < 0.01$, Fig. 5B and $p < 0.01$, Fig. 5C). Nevertheless, AAV-β-arrestin2 injection significantly decreased the level of phosphor-DARPP32/ERK proteins but not AAV-EGFP ($p < 0.01$, Fig. 5B and $p < 0.01$, Fig. 5C). In summary, our data indicated that AAV-β-arrestin2 regulated D1R, phosphor-DARPP32 and phosphor-ERK in the denervated striatum of LID rats.

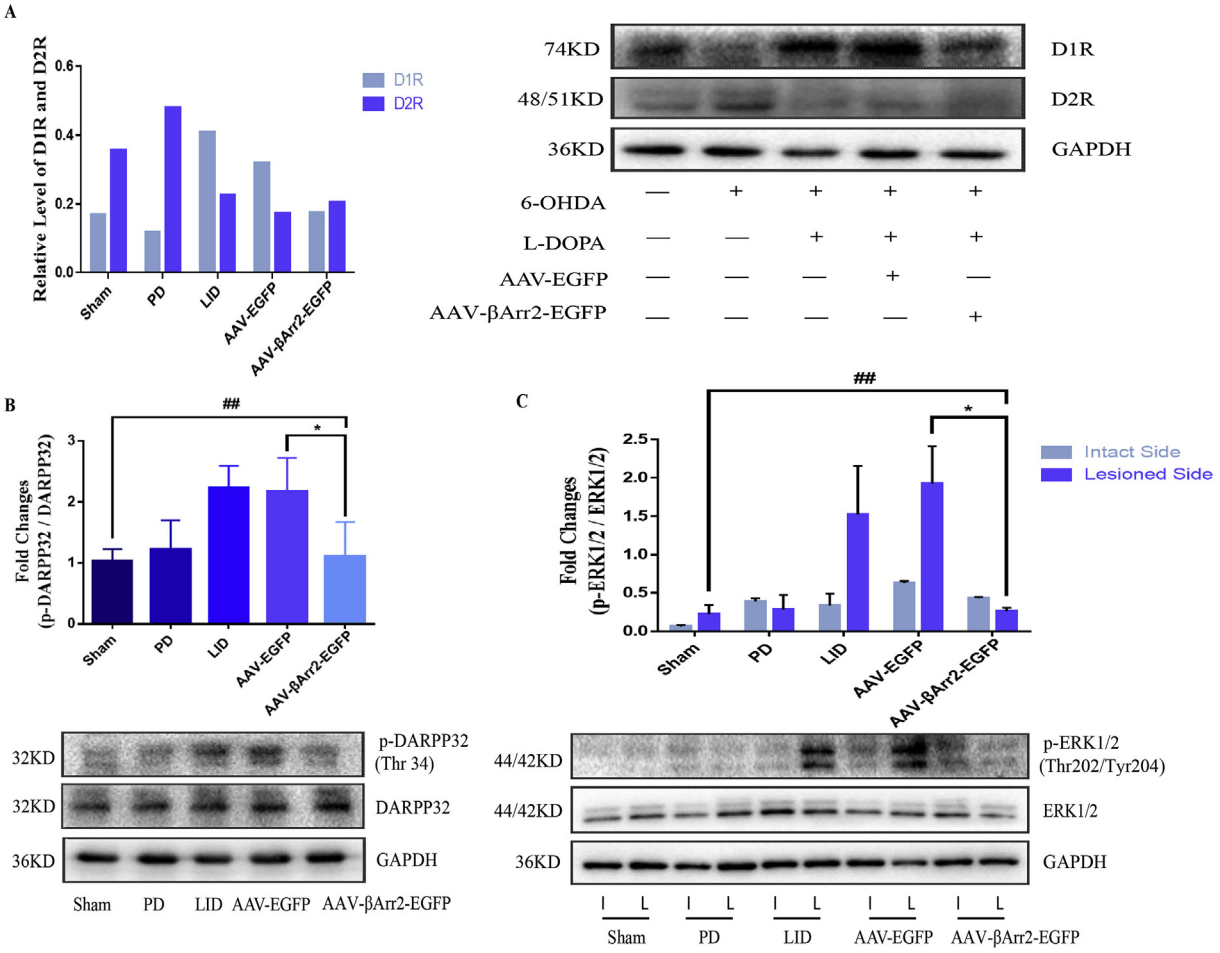


**Fig. 5.** AAV-Mediated β-arrestin2 overexpression blocks L-dopa-induced phosphor-DARPP32/.

### *3.4. AAV-mediated β-arrestin2 ablation potentiates AIMs induced by L-dopa*

To address the influence of striatal β-arrestin2 on AIMs, we generated AAV vectors encoding either a short hairpin RNA (shRNA) to block β-arrestin2 expression (AAV-sh. β-arrestin2) or a shRNA against firefly luciferase (AAV-sh. control) as a negative control. The infectivity of AAV-sh. β-arrestin2 was evaluated in 293T cells, indicating β-arrestin2 protein and mRNA expression were significantly decreased by AAV-sh. β-arrestin2 (H8249 + Y6738) compared to the control AAV-shRNA ($p < 0.05$, Fig. 6A and Fig. 6B). Analogously, in the rat's dorsal striatum, we found AAV-sh. β-arrestin2 (H8249 + Y6738) obviously decreased β-arrestin2 proteins ($p < 0.05$, Fig. 6C) and immunopositive neurons ($p < 0.05$, Fig. 6D) compared with other groups. AAV vectors were injected into the ipsilateral striatum, and the rats received daily therapy with L-dopa for 3 weeks to induce AIMs (Fig. 7A). Here, we showed that genetic deletion of β-arrestin2 (AAV-sh. β-arrestin2) significantly enhanced the dyskinesia-like effects of chronic L-dopa treatment in terms of ALO AIMs ($p < 0.05$, Fig. 7B and C), which was not found in the AAV-sh. control group ($p > 0.05$). We found this same trend in axial AIMs ($p < 0.05$, Fig. 7D), limb AIMs ($p < 0.05$, Fig. 7E) and orolingual AIMs ($p < 0.05$, Fig. 7F). Interestingly, there were no significant differences observed in FFT performance, suggesting that inhibition of striatal β-arrestin2 expression did not influence motor function in LID rats ($p > 0.05$, Fig. 7G).

### *3.5. AAV-mediated β-arrestin2 knock-down activates L-dopa-induced phosphor-DARPP32/ERK signaling in the lesioned striatum*

We further evaluated whether the viral deletion of β-arrestin2 affected D1R or D2R levels and found that both D1R and D2R protein levels were similar in the LID rats and the AAV-sh. β-arrestin2 rats (Fig. 8A), indicating that AAV-mediated β-arrestin2 knock-down had no obvious influence on the expression of the D1R and D2R. Moreover, we found that AAV-sh. β-arrestin2 significantly increased the level of phosphor-DARPP32 protein in the striatum compared with the LID group and the AAV-sh. control group (Fig. 8B). It has been demonstrated that L-dopa activates the ERK pathway. Thus, we examined the effect of chronic L-dopa treatment on the phosphorylation of ERK. As shown in Fig. 8C, there was a significant increase in phosphor-ERK proteins in the denervated striatum of AAV-sh. β-arrestin2 rats compared with other groups.

## 4. Discussion

LID represents one of the most disabling consequences of L-dopa replacement therapy for PD. The purpose of this study was to evaluate the role of β-arrestin2 specifically on the development of LID and the level of associated molecular markers in the denervated striatum of hemi-Parkinsonian rats. We reported here that β-arrestin2 protein affected the development of experimental LID via a direct pathway. In accordance with the low levels of β-arrestin2 in the lesioned dorsal striatum, we found that local AAV-mediated β-arrestin2 overexpression rats developed less severe AIM scores in response to L-dopa. This beneficial response was reversed by selective deletion of β-arrestin2 in

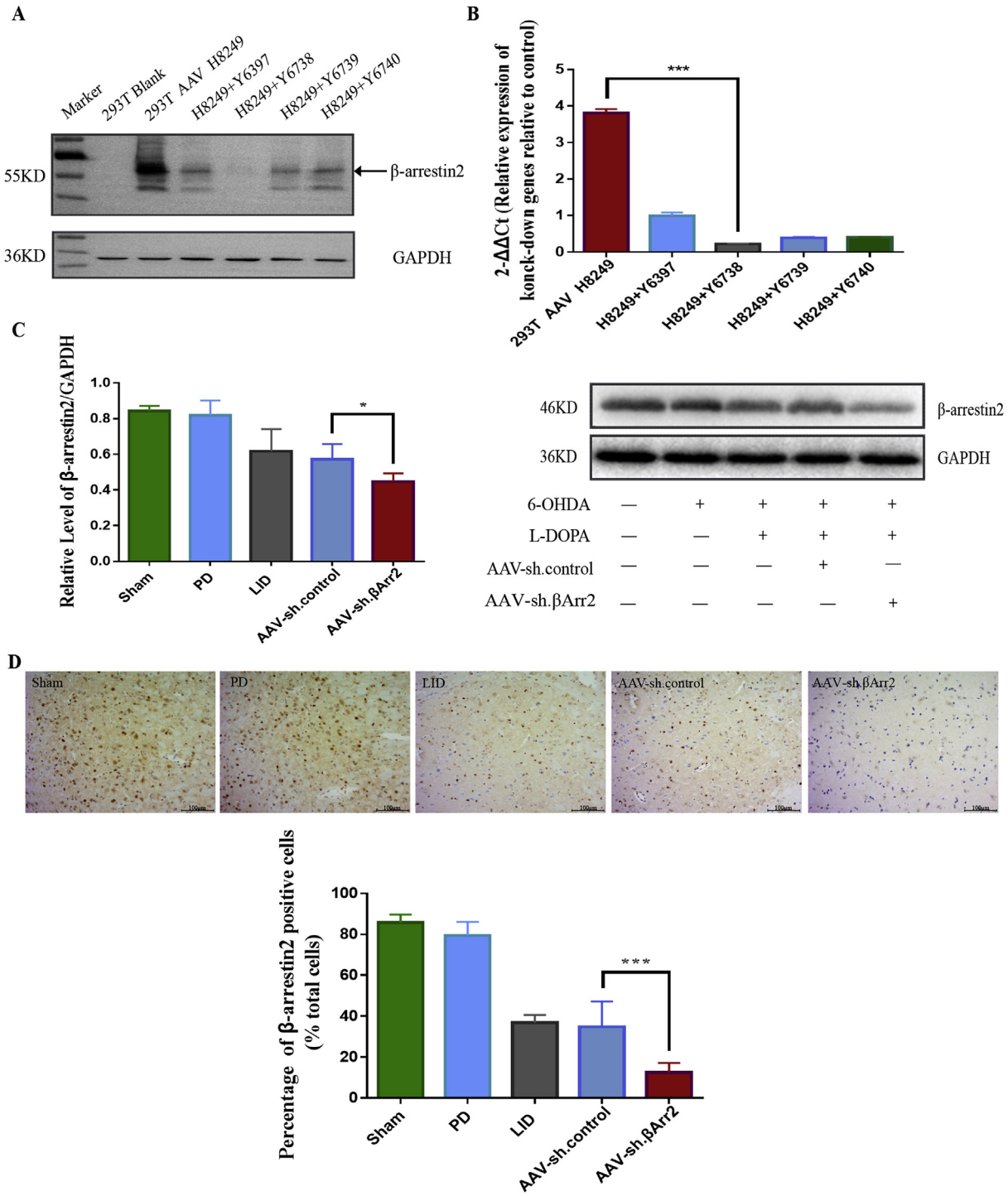


**Fig. 6.** AAV-mediated β-arrestin2 ablation in vitro and *in vivo*. (A) Detection of the AAV-sh. β-arrestin2 expression by WB in vitro; (B) Detection of the AAV-sh. β-arrestin2 expression by Q-PCR in vitro; (C) Detection of the AAV-sh. β-arrestin2 expression by WB in the lesioned rats striatum; (D) Detection of the AAV-sh. β-arrestin2 expression by IHC in the lesioned rats striatum. AAV-sh. β-arrestin2 (H8249 + Y6738) can decrease the β-arrestin2 proteins and immunopositive neurons compared with other groups (ANOVA followed by Bonferroni post hoc tests).

striatal neurons. These data indicated that AIMs developed with lower levels of β-arrestin2 but not with β-arrestin2 overexpression. Furthermore, no significant improvements in motor behavior (FFT) were seen in inhibition or overexpression of β-arrestin2. Our data were consistent with observations in one previous report (Urs et al., 2015), which demonstrated that either a genetic or pharmacological intervention to enhance β-arrestin2 expression could reduce dyskinesia behaviors. Moreover, we demonstrated that L-dopa treatment increased phosphor-DARPP32/ERK expression in direct D1R pathway neurons, and overexpression of β-arrestin2 diminished D1R protein and L-dopa-induced phosphor-DARPP32/ERK levels. Viral deletion of β-arrestin2 in LID rats markedly enhanced the dyskinesia-like effects of chronic L-dopa treatment and its key biochemical markers through a direct pathway.

TH is the enzyme that converts tyrosine into L-dopa, and a deficiency can present in Parkinsonism. In this paper, the extent of decline

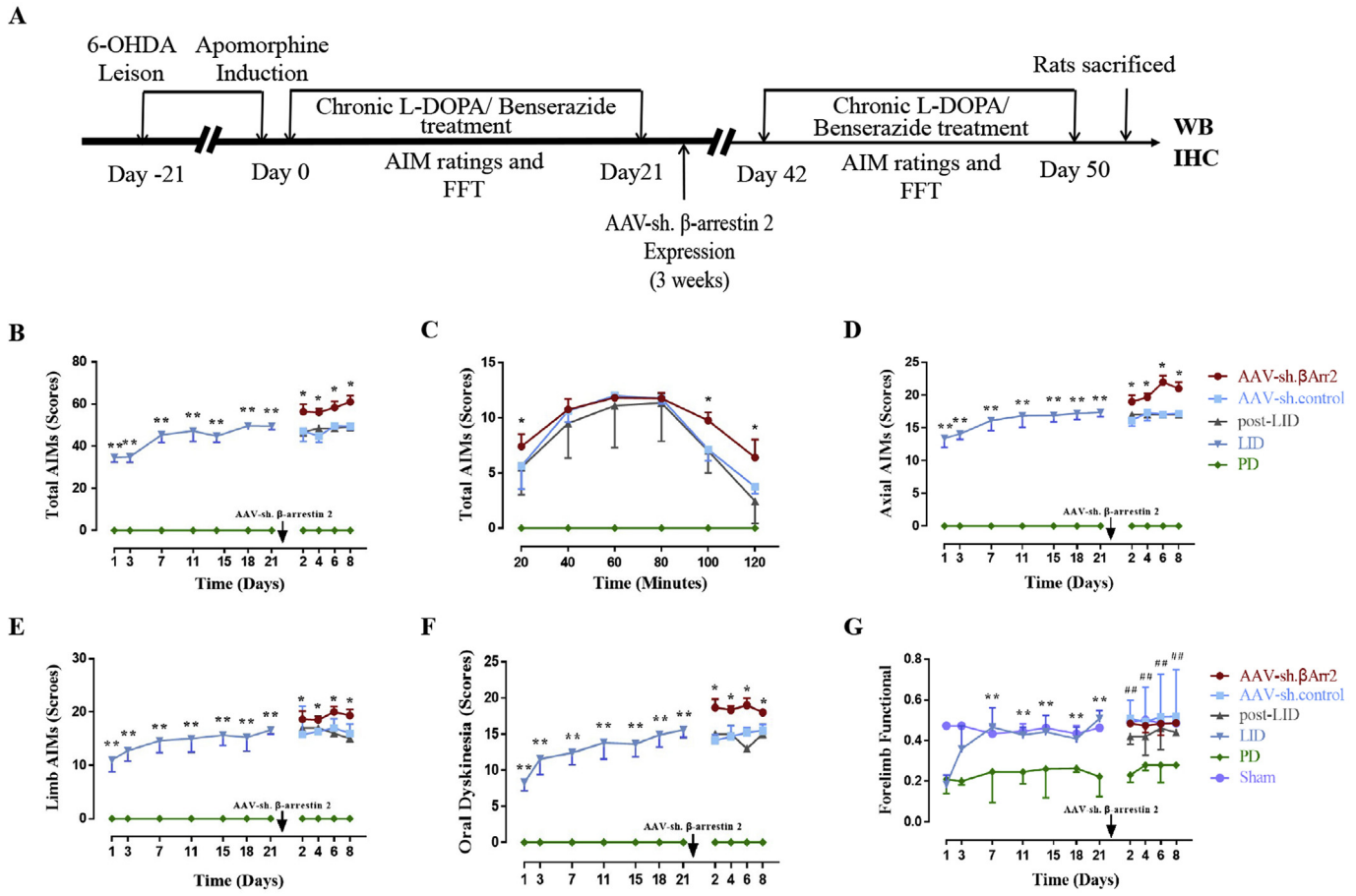


**Fig. 7.** AAV-Mediated β-arrestin2 ablation in striatum alters AIMs induced by L-dopa in 6-OHDA lesioned rats. (A) The protocol of the third part experimental design; (B–C) Total AIM score; (D) axial AIM score; (E) limb AIM score; (F) orolingual AIM score; (G) Forelimb functional test. We found that genetic deletion of β-arrestin2 (AAV-sh. β-arrestin2) significantly enhancing the dyskinesia-like effects of chronic L-dopa treatment in terms of AIM score without influence the active effects of L-dopa on parkinsonian motor scores. # $p < 0.05$ vs LD group; ## $p > 0.05$ vs LID group (n = 6 for each groups, Kruskal Wallis followed).

in 6-OHDA was verified by IFC and WB via the levels of TH. We found TH immunoreactive-(ir) neurons in the striatum were dramatically decreased by nearly 80%–90% in the PD rats compared with the sham group, which can be an indication of successfully establishing the PD model. Theoretically, the content of TH is limited in the striatum. Nevertheless, several researchers have shown that TH-ir neurons appeared in the striatum as early as 3 days after 6-OHDA lesion. One week after the lesion, the number of TH-ir neurons started to decrease, and this decrease progressed obviously over time (Darmopil et al., 2008). All striatal TH-ir neurons are projection neurons with direct and indirect striatal output pathways, and promotion of these striatal TH-ir neurons may be beneficial in PD (Jollivet et al., 2004). Critically, such striatal TH interneurons are not dopaminergic but rather are a type of GABAergic interneuron that expresses TH (Xenias et al., 2015). Accumulating evidence shows that LID occurs in response to the activation of sensitized D1R transmission in the MSNs of the striatum (Mosharov et al., 2015).

The pathological enlargement in the number of D1Rs at the membrane is likely to result in the development of LID and represents a potential target for therapeutic intervention due to uncontrolled downstream signals and neuronal activity. In line with this theory, recent findings have reported that LID is alleviated by promoting G-protein coupled receptor (GPCR) desensitization (Feyder et al., 2011; Nishi and Shuto, 2017). Strengthening β-arrestin2 function seems to be a suitable approach because β-arrestin2 is known to desensitize receptor signaling (Ismail et al., 2015). Mounting evidence indicates that β-arrestin2 unexpectedly function as scaffold proteins for many signaling elements in the cytoplasm and nucleus, thus regulating cellular responses and gene expression (Lefkowitz et al., 2006). Moreover, Nazish et al. reported that downregulation of a GPCR by β-arrestin2 mediated several mechanisms (Abdullah et al., 2016). In support of this assertion, in this study, we found AAV-induced β-arrestin2 overexpression in the dorsal striatum led to the disappearance of dyskinetic behaviors without interfering with the anti-Parkinsonian effect of L-dopa. Therefore, it has been supposed that enhancing β-Arrestin2 might alleviate the motor side effects induced by L-dopa. Conversely, AAV-shRNA-induced β-arrestin2 ablation results in worse AIM scores. Collectively, these findings are also supported by a previous study showing that β-Arrestin2 plays a crucial role in behavioral sensitization after L-dopa treatment (Urs et al., 2015; Dunn et al., 2016). However, the linkage between β-arrestin2 and LID is still insufficient despite the aforementioned results. We need more robust designs and experiments to confirm the relationship between β-arrestin2 and LID in the future, such as β-arrestin2 transgenic animals to explore this issue. The AIM score, which is a score commonly used to reflect behavioral sensitization to L-dopa, is caused by denervation-induced supersensitivity of the D1R in the dopamine-depleted striatum. On the other hand, based on our results, no obvious differences in motor behavior (FFT) were seen either in inhibition or overexpression of β-arrestin2, indicating that modified β-arrestin2 does not influence Parkinsonian motor symptoms. Conversely, Urs et al. reported that in the DDD/βarr2 KO mice, a drastically reduced and shortened locomotor response was observed, which has been suggested to reflect Parkinsonism. The reduction in the locomotor response in the DDD/βarr2 KO mice can be attributed to

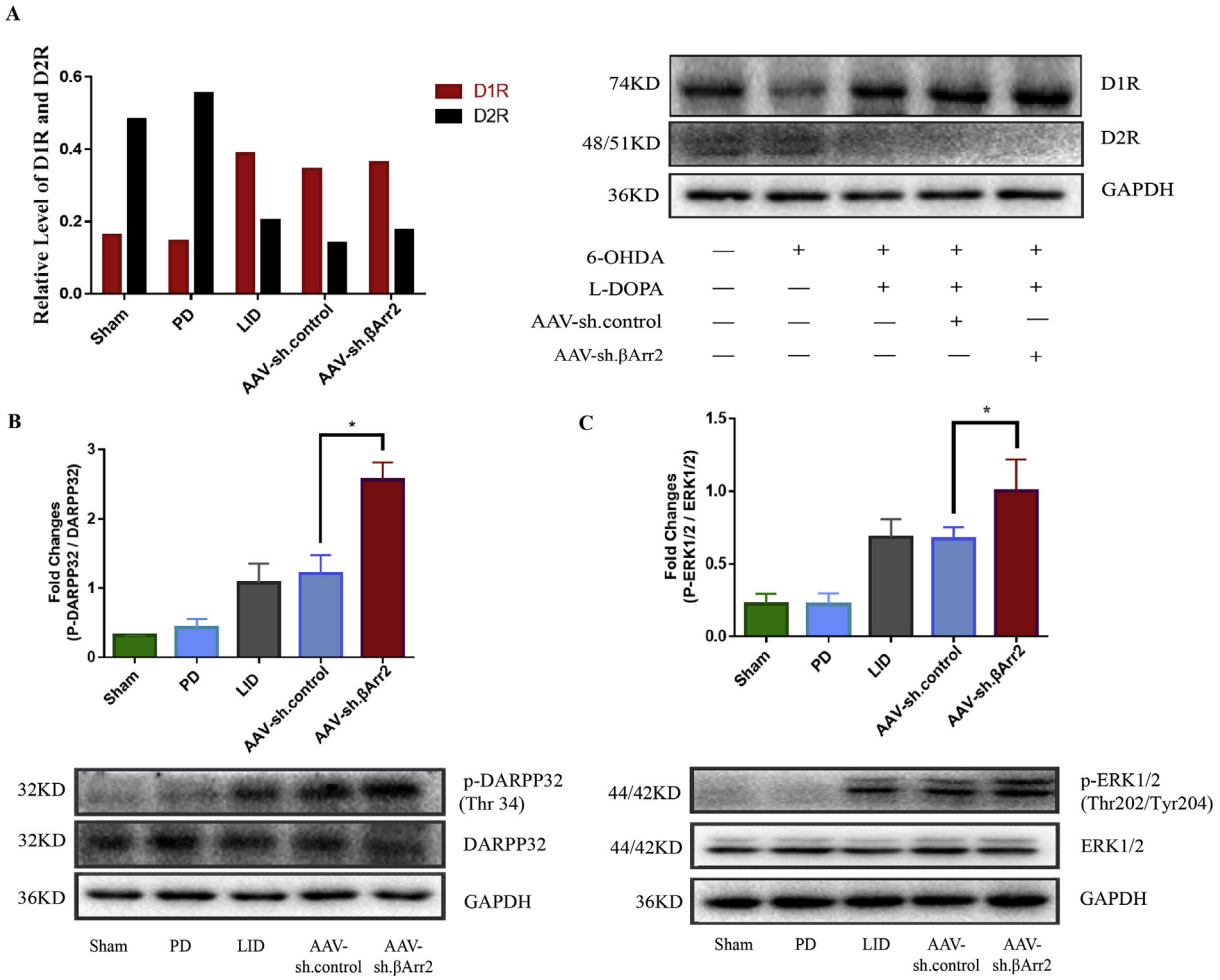


**Fig. 8.** AAV-mediated β-arrestin2 ablation activates L-dopa-induced phosphor-DARPP32/ERK signal in the lesioned striatum. (A) D1R and D2R protein levels relative to GAPDH; (B) phosphorylated DARPP32 (Thr34) level expressed relative to total DARPP32 level; (C) phosphorylated ERK (Thr202) level expressed relative to total ERK level. * $p < 0.01$ vs LID group and ## $p > 0.05$ vs LID group (ANOVA followed by Bonferroni post hoc tests).

genetic deletion of β-arrestin2 (Urs et al., 2015). We speculate that the discrepancy behind this paradoxical phenomenon is, in part, due to the different behavioral tests, which may influence the results even though both tests can reflect PD symptoms. In addition, the number of rats in each group was small and needs to be expanded to validate these results. Consequently, we should interpret these results with caution. More behavioral tests (such as the rotarod test, pole test and rotation test) modeling clinical symptoms of PD should be utilized in future research.

Although the exact molecular mechanisms of LID remain to be illuminated, exaggerated signaling of the striatal D1R has been involved in LID in rodents and primates, suggesting that normalization of this excessive signaling may be beneficial (Francardo and Cenci, 2014). Increased responsiveness of the D1R following sensitization to L-dopa gives rise to augmented synthesis of DARPP-32 (Håkansson et al., 2004). Pharmacological inhibition or genetic inactivation of DARPP-32 have been shown to reduce LID (Wan et al., 2017; Santini et al., 2007). Moreover, sensitized D1R-mediated transmission also activates ERK phosphorylation via activation of the PKA/DARPP-32 signaling cascade, which controls transcriptional and translational courses (Feyder et al., 2011; Cenci and Crossman, 2018). Inhibition of ERK signaling counteracts the development and expression of LID (Cerovic et al., 2015; Fasano et al., 2010), suggesting that ERK phosphorylation is also implicated in LID. Studies performed in PD rats show that depletion of striatal dopamine confers the ability to increase the phosphorylation of ERK to a D1R agonist (Gerfen et al., 2002). Therefore, the function of ERK is likely dependent on sensitized D1R-mediated transmission and abnormal activation of cAMP signaling, indicating ERK is downstream of D1R in the LID mechanism. In addition, we found that the mechanism of β-arrestin2 was likely through the reduction of the D1R-mediated signaling pathway in LID, including the inhibition of ERK activation. Unfortunately, the causal link between ERK and β-arrestin2 through D1R activity was not directly tested in this paper. Furthermore, β-arrestin2 have also been found to play novel roles in regulating intracellular signaling networks related to malignant cell functions, including ERK, JNK, and others (Luttrell and Gesty-Palmer, 2010; Luttrell, 2013). Our data demonstrated that accelerating GPCR desensitization in the dopamine-depleted striatum via virus-mediated overexpression of β-arrestin2 relieved LID in rodent models. In 6-OHDA-lesioned hemi-Parkinsonian rats, we found that β-arrestin2 promoted D1R internalization and suppressed L-dopa–induced activation of phosphor-DARPP32 and phosphor-ERK attributed to attenuated D1R signaling. Thus, the pattern of behavioral and molecular mechanisms supports the conclusion that β-arrestin2 overexpression relieved LID by increasing desensitization of D1R. However, the link between β-arrestin2 and D1R signaling in this research is weak. The hyperactivity of D1R in LID does not equal an increase in D1R protein levels. Currently, we are unable to clearly conclude that β-arrestin2 acted in LID by reducing D1R-mediated signaling. Consequently, we need to use genetic or pharmacological inhibition of D1R/DARPP32/ERK signaling to further elucidate the relationship between β-arrestin2 and the D1R signaling pathway in future. Further studies are also

needed to elucidate the beneficial effects of β-arrestin2 derived from MSN cell types, and we will investigate this topic in the future with transgenic mice with striatum-specific overexpression or ablation of β-Arrestin2.

Our results demonstrated that targeted enhancement of GPCR desensitization substantially relieved LID in 6-OHDA-lesioned PD animal models through β-arrestin2. Moreover, the absence of β-arrestin2 enhanced LID behaviors. This amelioration of LID did not compromise the anti-Parkinsonian benefits of L-dopa, offering hope of achieving the elusive goal of controlling LID behaviors. In addition, we found that β-arrestin2 treatment prevented the development of LID by inhibiting the expression of phosphor-DARPP32 and phosphor-ERK in dyskinetic rats.

## Conflict of interests

The authors declare that the research was conducted in the absence of any commercial or financial relationships that could be construed as a potential conflict of interest.

## Authors' contributions

ZRZ made substantial contributions to conception and design. XRZ and WWW analyzed the data and helped to revise the manuscript. XSW and XYW helped to response the comments and replenished the required data. XQR helped to revise the manuscript. CLX and BS were involved in drafting the manuscript. All authors read and approved the final manuscript.

## Funding statement

The study was supported by the Projects of National Science Foundation of China (No. 81600977) and the Projects of Wenzhou city Committee of Science and Technology (Y20170067 and Y20180137) and the Projects of Natural Science Foundation of Zhejiang Province (Y19H090059), as well as Zhejiang Science and Technology Plan Project (2017C37106) and Zhejiang Medical and Health Science and Technology Project (2015DTA017).

## Acknowledgments

The authors would like to thank Prof Xin-Shi Wang for supporting his work and performing the statistical analysis and language improvement of the paper.

## Appendix A. Supplementary data

Supplementary data to this article can be found online at https://doi.org/10.1016/j.neuint.2019.104543.

ERK signal in the lesioned striatum. They were assessed in extracts from 6-OHDA-lesioned rats treated with vehicle, pulsatile L-dopa (15 mg/kg) plus benserazide (3.75 mg/kg), AAV-β-arrestin2-EGFP and AAV-EGFP. (A) D1R and D2R protein levels relative to GAPDH; (B) phosphorylated DARPP32 (Thr34) level expressed relative to total DARPP32 level; (C) phosphorylated ERK (Thr202) level expressed relative to total ERK level, Protein levels were evaluated by WB extracted from the striatum ipsilateral to the 6-OHDA lesion. * $p < 0.01$ vs LID group and ## $p > 0.05$ vs LID group (ANOVA followed by Bonferroni post hoc tests).

## References

Abdullah, N., Beg, M., Soares, D., Dittman, J.S., McGraw, T.E., 2016. Downregulation of a GPCR by β-arrestin2-mediated switch from an endosomal to a TGN recycling pathway. Cell Rep. 17, 2966–2978. https://doi.org/10.1016/j.celrep.2016.11.050.

Antonini, A., Tinazzi, M., 2015. Targeting pain in Parkinson's disease. Lancet Neurol. 14, 1144–1145. https://doi.org/10.1016/S1474-4422(15)00286-0.

Bohn, L.M., Gainetdinov, R.R., Sotnikova, T.D., Medvedev, I.O., Lefkowitz, R.J., Dykstra, L.A., Caron, M.G., 2003. Enhanced rewarding properties of morphine, but not cocaine, in beta(arrestin)-2 knock-out mice. J. Neurosci. 23, 10265–10273.

Brugnoli, A., Napolitano, F., Usiello, A., Morari, M., 2016. Genetic deletion of Rhes or pharmacological blockade of mTORC1 prevent striato-nigral neurons activation in levodopa-induced dyskinesia. Neurobiol. Dis. 85, 155–163. https://doi.org/10.1016/j.nbd.2015.10.020.

Bruns, I.R., Chhum, S., Dinh, A.T., Doerr, H., Dunn, N.R., Ly, Y.T., Mitman, C.L., Rickards, H.D., Sol, C., Wan, E.W., Raffa, R.B., 2006. A potential novel strategy to separate therapeutic- and side-effects that are mediated via the same receptor: beta-arrestin2/G-protein coupling antagonists. J. Clin. Pharm. Ther. 31, 119–128. https://doi.org/10.1111/j.1365-2710.2006.00714.x.

Cenci, M.A., Crossman, A.R., 2018. Animal models of l-dopa-induced dyskinesia in Parkinson's disease. Mov. Disord. 33, 889–899. https://doi.org/10.1002/mds.27337. 10.1002/mds.27337.

Cenci, M.A., Lee, C.S., Björklund, A., 1998. L-DOPA-induced dyskinesia in the rat is associated with striatal overexpression of prodynorphin- and glutamic acid decarboxylase mRNA. Eur. J. Neurosci. 10, 2694–2706. https://doi.org/10.1038/srep07506.

Cerovic, M., Bagetta, V., Pendolino, V., Ghiglieri, V., Fasano, S., Morella, I., Hardingham, N., Heuer, A., Papale, A., Marchisella, F., Giampà, C., Calabresi, P., Picconi, B., Brambilla, R., 2015. Derangement of Ras-guanine nucleotide-releasing factor 1 (Ras-GRF1) and extracellular signal-regulated kinase (ERK) dependent striatal plasticity in L-DOPA-induced dyskinesia. Biol. Psychiatry 77, 106–115. https://doi.org/10.1016/j.biopsych.2014.04.002.

Cotzias, G.C., Van, Woert, M.H., Schiffer, L.M., 1967. Aromatic amino acids and modification of parkinsonism. N. Engl. J. Med. 276, 374–379.

Darmopil, S., Muñetón-Gómez, V.C., de, Ceballos, M.L., Bernson, M., Moratalla, R., 2008. Tyrosine hydroxylase cells appearing in the mouse striatum after dopamine denervation are likely to be projection neurones regulated by L-DOPA. Eur. J. Neurosci. 27, 580–592.

Dunn, H.A., Chahal, H.S., Caetano, F.A., Holmes, K.D., Yuan, G.Y., Parikh, R., Heit, B., Ferguson, S.S.G., 2016. PSD-95 regulates CRFR1 localization, trafficking and β-arrestin2 recruitment. Cell. Signal. 28, 531–540. https://doi.org/10.1016/j.cellsig.2016.02.013.

Fasano, S., Bezard, E., D'Antoni, A., Francardo, V., Indrigo, M., Qin, L., Doveró, S., Cerovic, M., Cenci, M.A., Brambilla, R., 2010. Inhibition of Ras-guanine nucleotide-releasing factor 1 (Ras-GRF1) signaling in the striatum reverts motor symptoms associated with L-dopa-induced dyskinesia. Proc. Natl. Acad. Sci. U.S.A. 107, 21824–21829. https://doi.org/10.1073/pnas.1012071107.

Feyder, M., Bonito-Oliva, A., Fisone, G., 2011. L-DOPA-Induced dyskinesia and abnormal signaling in striatal medium spiny neurons: focus on dopamine D1 receptor-mediated transmission. Front. Behav. Neurosci. 5, 71. https://doi.org/10.3389/fnbeh.2011.00071.

Feyder, M., Södersten, E., Santini, E., Vialou, V., LaPlant, Q., Watts, E.L., 2016. A role for mitogen- and stress-activated kinase 1 in L-DOPA-induced dyskinesia and ΔFosB expression. Biol. Psychiatry 79, 362–371. https://doi.org/10.1016/j.biopsych.2014.07.019.

Francardo, V., Cenci, M.A., 2014. Investigating the molecular mechanisms of L-DOPA-induced dyskinesia in the mouse. Park. Relat. Disord. 20 (Suppl. 1), S20–S22. https://doi.org/10.1016/S1353-8020(13)70008-7.

Gerfen, C.R., Miyachi, S., Paletzki, R., Brown, P., 2002. D1 dopamine receptor supersensitivity in the dopamine-depleted striatum results from a switch in the regulation of ERK1/2/MAP kinase. J. Neurosci. 22, 5042–5054.

Håkansson, K., Lindskog, M., Pozzi, L., Usiello, A., Fisone, G., 2004. DARPP-32 and modulation of cAMP signaling: involvement in motor control and levodopa-induced dyskinesia. Park. Relat. Disord. 10, 281–286. https://doi.org/10.1016/j.parkreldis.2004.02.010.

Ismail, S., Dubois-Vedrenne, I., Laval, M., Tikhonova, I.G., D'Angelo, R., Sanchez, C., Clerc, P., Gherardi, M.J., Gigoux, V., Magnan, R., Fourmy, D., 2015. Internalization and desensitization of the human glucose-dependent-insulinotropic receptor is affected by N-terminal acetylation of the agonist. Mol. Cell. Endocrinol. 414, 202–215. https://doi.org/10.1016/j.mce.2015.07.001.

Jollivet, C., Montero-Menei, C.N., Venier-Julienne, M.C., Sapin, A., Benoit, J.P., Menei, P., 2004. Striatal tyrosine hydroxylase immunoreactive neurons are induced by L-dihydroxyphenylalanine and nerve growth factor treatment in 6-hydroxydopamine lesioned rats. Neurosci. Lett. 362, 79–82.

Lee, M.H., Appleton, K.M., Strungs, E.G., Kwon, J.Y., Morinelli, T.A., Peterson, Y.K., Laporte, S.A., Luttrell, L.M., 2016. The conformational signature of β-arrestin2 predicts its trafficking and signalling functions. Nature 531, 665–669. https://doi.org/10.1038/nature17154.

Lefkowitz, R.J., Rajagopal, K., Whalen, E.J., 2006. New roles for beta-arrestins in cell signaling: not just for seven-transmembrane receptors. Mol. Cell 24, 643–652. https://doi.org/10.1016/j.molcel.2006.11.007.

Lohse, M.J., Benovic, J.L., Codina, J., Caron, M.G., Lefkowitz, R.J., 1990. beta-Arrestin: a protein that regulates beta-adrenergic receptor function. Science 248, 1547–1550.

Lundblad, M., Vaudano, E., Cenci, M.A., 2003. Cellular and behavioural effects of the adenosine A2a receptor antagonist KW-6002 in a rat model of l-DOPA-induced dyskinesia. J. Neurochem. 84, 1398–1410.

Luttrell, L.M., 2013. Arrestin pathways as drug targets. Prog. Mol. Biol. Transl. Sci. 118, 469–497. https://doi.org/10.1016/B978-0-12-394440-5.00018-8.

Luttrell, L.M., Gesty-Palmer, D., 2010. Beyond desensitization: physiological relevance of arrestin-dependent signaling. Pharmacol. Rev. 62, 305–330. https://doi.org/10.1124/pr.109.002436.

Mosharov, E.V., Borgkvist, A., Sulzer, D., 2015. Presynaptic effects of levodopa and their possible role in dyskinesia. Mov. Disord. 30, 45–53. https://doi.org/10.1002/mds.26103.

Nishi, A., Shuto, T., 2017. Potential for targeting dopamine/DARPP-32 signaling in

neuropsychiatric and neurodegenerative disorders. Expert Opin. Ther. Targets 21, 259–272. https://doi.org/10.1080/14728222.2017.1279149.
Pavón, N., Martín, A.B., Mendialdua, A., Moratalla, R., 2006. ERK phosphorylation and FosB expression are associated with L-DOPA-induced dyskinesia in hemiparkinsonian mice. Biol. Psychiatry 59, 64–74.
Santini, E., Valjent, E., Usiello, A., Carta, M., Borgkvist, A., Girault, J.A., Hervé, D., Greengard, P., Fisone, G., 2007. Critical involvement of cAMP/DARPP-32 and extracellular signal-regulated protein kinase signaling in L-DOPA-induced dyskinesia. J. Neurosci. 27, 6995–7005. https://doi.org/10.1523/JNEUROSCI.0852-07.2007.
Santini, E., Sgambato-Faure, V., Li, Q., Savasta, M., Dovero, S., Fisone, G., 2010. Distinct changes in cAMP and extracellular signal-regulated protein kinasesignalling in L-DOPA-induced dyskinesia. PLoS One 5, e12322. https://doi.org/10.1371/journal.pone.0012322.
Schaeffer, E., Pilotto, A., Berg, D., 2014. Pharmacological strategies for the management of levodopa-induced dyskinesia in patients with Parkinson's disease. CNS Drugs 28, 1155–1184. https://doi.org/10.1007/s40263-014-0205-z.
Schallert, T., Fleming, S.M., Leasure, J.L., Tillerson, J.L., Bland, S.T., 2000. CNS plasticity and assessment of forelimb sensorimotor outcome in unilateral rat models of stroke, cortical ablation, parkinsonism and spinal cord injury. Neuropharmacology 39, 777–787.
Stocchi, F., Tagliati, M., Olanow, C.W., 2008. Treatment of levodopa-induced motor complications. Mov. Disord. 23, S599–S612. https://doi.org/10.1002/mds.22052.
Urs, N.M., Bido, S., Peterson, S.M., Daigle, T.L., Bass, C.E., Gainetdinov, R.R., Bezard, E., Caron, M.G., 2015. Targeting β-arrestin2 in the treatment of L-DOPA-induced dyskinesia in Parkinson's disease. Proc. Natl. Acad. Sci. U.S.A. 112, E2517–E2526. https://doi.org/10.1073/pnas.1502740112.
Valjent, E., Pascoli, V., Svenningsson, P., Paul, S., Enslen, H., Corvol, J.C., 2005. Regulation of a protein phosphatase cascade allows convergent dopamine and glutamate signals to activate ERK in the striatum. Proc. Natl. Acad. Sci. *U.S.A.* 102, 491–496.
Wan, Y., Wu, N., Song, L., Wang, X., Liu, Z., Yuan, W., 2017. Levodopa/benserazide loaded microspheres alleviate L-dopa induced dyskinesia through preventing the over-expression of D1R/shp-2/ERK1/2 signaling pathway in a rat model of Parkinson's disease. Front. Aging Neurosci. 9, 331. https://doi.org/10.3389/fnagi.2017.00331.
Xenias, H.S., Ibáñez-Sandoval, O., Koós, T., Tepper, J.M., 2015. Are striatal tyrosine hydroxylase interneurons dopaminergic? J. Neurosci. 35, 6584–6599.
Xie, C.L., Wang, W.W., Zhang, S.F., Yuan, M.L., Che, J.Y., Gan, J., Liu, Z.G., 2014. Levodopa/benserazide microsphere (LBM) prevents L-dopa induced dyskinesia by inactivation of the DR1/PKA/P-tau pathway in 6-OHDA-lesioned Parkinson's rats. Sci. Rep. 4, 7506.
Xie, C.L., Lin, J.Y., Wang, M.H., Zhang, Y., Zhang, S.F., Wang, X.J., Liu, Z.G., 2016. Inhibition of Glycogen Synthase Kinase-3β (GSK-3β) as potent therapeutic strategy to ameliorates L-dopa-induced dyskinesia in 6-OHDA parkinsonian rats. Sci. Rep. 6, 23527. https://doi.org/10.1038/srep23527.
Zhan, X., Gimenez, L.E., Gurevich, V.V., Spiller, B.W., 2011. Crystal structure of arrestin-3 reveals the basis of the difference in receptor binding between two non-visual subtypes. J. Mol. Biol. 406, 467–478. https://doi.org/10.1016/j.jmb.2010.12.034.